

PESSTO monitoring of SN 2012hn: further heterogeneity among faint type I supernovae^{*}

S. Valenti^{1,2} †, F. Yuan^{3,4}, S. Taubenberger⁵, K. Maguire⁶, A. Pastorello⁷, S. Benetti⁷, S. J. Smartt⁸, E. Cappellaro⁷, D. A. Howell^{1,2}, L. Bildsten^{2,9}, K. Moore², M. Stritzinger¹⁰, J. P. Anderson¹¹, S. Benitez-Herrera⁵, F. Bufano¹², S. Gonzalez-Gaitan¹¹, M. G. McCrum⁸, G. Pignata¹², M. Fraser⁸, A. Gal-Yam¹³, L. Le Guillou¹⁴, C. Inserra⁸, D. E. Reichart¹⁵, R. Scalzo³, M. Sullivan¹⁶, O. Yaron¹³, D. R. Young⁸

¹ *Las Cumbres Observatory Global Telescope Network, 6740 Cortona Dr., Suite 102, Goleta, CA 93117, USA*

² *Department of Physics, University of California, Santa Barbara, Broida Hall, Mail Code 9530, Santa Barbara, CA 93106-9530, USA*

³ *Research School of Astronomy and Astrophysics, The Australian National University, Weston Creek, ACT 2611, Australia*

⁴ *ARC Centre of Excellence for All-sky Astrophysics (CAASTRO)*

⁵ *Max-Planck-Institut für Astrophysik, Karl-Schwarzschild-Str. 1, 85741 Garching bei München, Germany*

⁶ *Department of Physics (Astrophysics), University of Oxford, DWB, Keble Road, Oxford, OX1 3RH, UK*

⁷ *INAF Osservatorio Astronomico di Padova, Vicolo dell'Osservatorio 5, 35122 Padova, Italy*

⁸ *Astrophysics Research Centre, School of Mathematics and Physics, Queens University Belfast, Belfast BT7 1NN, UK*

⁹ *Kavli Institute for Theoretical Physics, Kohn Hall, University of California, Santa Barbara, CA 93106-4030, USA*

¹⁰ *Department of Physics and Astronomy, Aarhus University, Ny Munkegade 120, DK-8000 Aarhus C, Denmark*

¹¹ *Departamento de Astronomia, Universidad de Chile, Casilla 36-D, Santiago, Chile*

¹² *Departamento de Ciencias Físicas, Universidad Andres Bello, Avda. Republica 252, Santiago, Chile*

¹³ *Department of Particle Physics and Astrophysics, The Weizmann Institute of Science, Rehovot 76100, Israel*

¹⁴ *UPMC Univ. Paris 06, UMR 7585, Laboratoire de Physique Nucleaire et des Hautes Energies (LPNHE), 75005 Paris, France*

¹⁵ *University of North Carolina at Chapel Hill, Campus Box 3255, Chapel Hill, NC 27599-3255, USA*

¹⁶ *School of Physics and Astronomy, University of Southampton, Southampton, SO17 1BJ, UK*

Accepted; Received; in original form

ABSTRACT

We present optical and infrared monitoring data of SN 2012hn collected by the Public ESO Spectroscopic Survey for Transient Objects (PESSTO). We show that SN 2012hn has a faint peak magnitude ($M_R \sim -15.7$) and shows no hydrogen and no clear evidence for helium in its spectral evolution. Instead, we detect prominent Ca II lines at all epochs, which relates this transient to previously described ‘Ca-rich’ or ‘gap’ transients. However, the photospheric spectra (from -3 to $+32$ d with respect to peak) of SN 2012hn show a series of absorption lines which are unique, and a red continuum that is likely intrinsic rather than due to extinction. Lines of Ti II and Cr II are visible. This may be a temperature effect, which could also explain the red photospheric colour. A nebular spectrum at $+150$ d shows prominent Ca II, O I, C I and possibly Mg I lines which appear similar in strength to those displayed by core-collapse SNe. To add to the puzzle, SN 2012hn is located at a projected distance of 6 kpc from an E/S0 host and is not close to any obvious starforming region. Overall SN 2012hn resembles a group of faint H-poor SNe that have been discovered recently and for which a convincing and consistent physical explanation is still missing. They all appear to explode preferentially in remote locations offset from a massive host galaxy with deep limits on any dwarf host galaxies, favouring old progenitor systems. SN 2012hn adds heterogeneity to this sample of objects. We discuss potential explosion channels including He-shell detonations and double detonations of white dwarfs as well as peculiar core-collapse SNe.

Key words: supernovae: general – supernovae: SN 2012hn – galaxies: NGC 2272

1 INTRODUCTION

Over the past few years, an increasing number of transients with unusual properties have been studied. In particular, a wide group of peculiar hydrogen-free supernovae (SNe) has been linked to hypothetical explosion channels that may not be due to the canonical mechanisms of iron core collapse or thermonuclear explosions of a near-Chandrasekhar-mass white dwarfs (e.g. SN 2008ha: Valenti et al. 2009; Foley et al. 2009; SN 2005E: Perets et al. 2010; SN 2002bj: Poznanski et al. 2010; SN 2010X: Kasliwal et al. 2010; SN 2005cz: Kawabata et al. 2010; PTF09dav: Kasliwal et al. 2012; Sullivan et al. 2011; SN 2010et/PTF10iuv¹: Kasliwal et al. 2012).

Several authors have grouped these objects into new classes: ‘SNe Iax’ (Foley et al. 2012); ‘rapidly declining SNe’ (Poznanski et al. 2010); ‘Ca-rich transients’ (Filippenko et al. 2003; Perets et al. 2010). The class of SNe Iax includes objects with spectra similar to SN 2002cx. SN 2008ha may be an extreme low-velocity member of this class, while SNe 2002bj and 2010X are the two members of the rapid-decay SN class (Kasliwal et al. 2010). In this paper we will focus on the ‘Ca-rich transients’. These are usually faint type I SNe, which reach peak absolute magnitudes of $M_R \geq -16$ and exhibit photospheric expansion velocities of $\sim 11000 \text{ km s}^{-1}$. They preferentially occur in the outskirts of their presumed host galaxies (Perets et al. 2010; Kasliwal et al. 2012) and their designation stems from prevalent calcium lines that dominate soon after maximum². Members of this group are SN 2005E, SN 2005cz, SN 2010et and PTF11bj.

The detection of strong calcium lines is not a unique property of this group of SNe, since these are occasionally detected in other SN types as well. For example, faint type IIP SNe also exhibit strong calcium lines at late phases (Pastorello et al. 2004). Similarly, SN 2008ha shows strong Ca lines. However, this SN was very faint, evolved rapidly, had a remarkably low photospheric velocity and spectra different from all other Ca-rich objects. Since the detection of strong Ca features may be common to different SN types, we will instead refer to these objects as faint type I SNe.

Presented in this paper are observations of the faint Type I SN 2012hn, acquired by the Public ESO Spectroscopic Survey for Transient Objects (PESSTO³). The overall science goal of PESSTO is to provide a public data base of high-quality optical + near-infrared (NIR) spectral time series of 150 optical transients covering the full parameter

¹ SN 2010et was discovered by Drake et al. (2010) and independently, but never announced, by the Palomar Transient Factory (PTF, Rau et al. 2009).

² In the case of SN 2005E, a spectral model for a not completely nebular spectrum was presented by Perets et al. (2010). These authors inferred a calcium abundance much larger than ever seen in other SNe. This result has not been confirmed yet for other Ca-rich transients.

³ In response to the first call by the European Southern Observatory (ESO) for public spectroscopic surveys, and particularly prompted by the opportunities provided by currently running wide-field surveys, PESSTO was awarded 90 nights per year on the New Technology Telescope (NTT) for four years, with continuation dependent on a mid-term review and the possibility for a fifth year of operations depending on the future of La Silla.

space that modern surveys deliver in terms of luminosity, host metallicity and explosion mechanisms. SN 2012hn is a PESSTO Key Science target as it conforms with the science goal to study unusual and unexplained transients.

The data will be presented and compared with other SNe belonging to the class of faint type I SNe: SN 2005E, SN 2005cz, SN 2010et and PTF11bj. Kasliwal et al. (2012) included in this class also PTF09dav (Sullivan et al. 2011) and SN 2007ke (Filippenko et al. 2007), and identified possible other class members in archival data.

PTF09dav is the only object within this group that spectroscopically resembles 1991bg-like SNe Ia, but with scandium and strontium features in photospheric spectra (Sullivan et al. 2011), and weak hydrogen emission during the nebular phase (Kasliwal et al. 2012). It was initially identified as a peculiar sub-luminous SN Ia (Sullivan et al. 2011) and later included by Kasliwal et al. (2012) in the group of Ca-rich transients. SN 2007ke has been added on the basis of a strong feature at 7300 Å identified as [Ca II] $\lambda\lambda 7291, 7323$ in a spectrum 19 days after maximum.

Whenever possible, PTF09dav and SN 2007ke have been included in the discussion even though their link with the other objects is less secure. The other possible members of this class, identified in archival data, are not included in this paper. The lack of quality data for most of them makes it even more difficult to establish their physical link with the group of faint type I SNe. Some of the SNe Iax, recently presented by Foley et al. (2012), are in principle faint type I SNe, but their spectra are quite different and we do not discuss them here.

2 DATA

SN 2012hn was discovered by the Catalina Real-Time Transient Survey (CRTS) on 2012 March 12.43 (UT dates are used throughout this paper) and classified at the ESO-NTT on 2012 March 14.02 as a peculiar SN Ic with some unidentified features (Benitez-Herrera et al. 2012) during an ELP⁴ observing run. No objects with similar spectra were identified in the Padova Supernova archive, making SN 2012hn an interesting and rare type of SN.

Given its right ascension (see next section), SN 2012hn could be followed only for ~ 2 months after discovery. We collected 4 spectra with NTT+EFOSC2 in April and two spectra (with VLT+XSHOOTER and Magellan+LDSS3) in May. Two nebular spectra were obtained with VLT+XSHOOTER on 2012 September 13.37 and September 14.37. Photometry was collected mostly with NTT+EFOSC2 and the PROMPT 5 telescope (Reichart et al. 2005), with a handful of points added by the TRAPPIST and Du Pont telescopes. The log of our spectroscopic observations of SN 2012hn is reported in Table 1, the photometry in Tables A1 and A2.

The NTT spectra were reduced using a custom-built PYTHON/PYRAF package developed by the author to reduce PESSTO data. Spectral reduction within the NTT pipeline includes corrections for bias and fringing, wavelength and

flux calibration, correction for telluric absorptions and a check on the correctness of the wavelength calibration using the atmospheric emission lines. The VLT+XSHOOTER spectra were reduced using the ESO-XSHOOTER pipeline version 1.0.0 under the GASGANO framework. The Magellan+LDSS3 spectrum was reduced in a standard fashion using IRAF. Imaging data were reduced using the QUBA pipeline (see Valenti et al. 2011). The SN photometry was measured through PSF fitting and calibrated against a set of local sequence stars. The latter were calibrated with respect to Landolt and Sloan standard fields during two photometric nights at the NTT. The magnitude errors account for the uncertainties in the PSF fit and the zero points (photometric calibration). The magnitudes of the local sequence stars are reported in Tables A3 (Landolt system) and A4 (Sloan system). Our spectral sequence and light curves are shown in Fig. 1.

Already in the first spectrum, SN 2012hn showed prominent lines that are usually observed in SNe with relatively low temperatures. The spectra are red with a drop in luminosity below 5300 Å that yields a SN $B - V$ colour ~ 2 . The B band evolves much faster than other optical bands, and its peak likely occurred earlier than the discovery. Whether SN 2012hn is intrinsically very red or it is red because of dust extinction along the line of sight is not obvious. Unfortunately, for this kind of transients a robust method to estimate the extinction does not exist. For this reason, in the next section we will discuss different reddening scenarios.

3 HOST AND REDDENING

SN 2012hn is located at $\alpha = 06^{\text{h}}42^{\text{m}}42^{\text{s}}.55$ and $\delta = -27^{\circ}26'49''.8$, 44.2 arcsec north and 18.7 arcsec east of the nucleus of NGC 2272, an E/S0-type galaxy⁵ (see Fig. 2 and Table 2). Assuming a distance of 26.8 ± 1.9 Mpc for NGC 2272⁶, SN 2012hn lies at a projected distance of 6.2 kpc from the centre of the host. To compare the SN location against the host-galaxy light / stellar-mass distribution, we estimate the enclosed light fraction using the following method: we model the projected radial surface density profile of the host galaxy using fluxes extracted in elliptical apertures and calculate the ratio of light within the ellipse defined by the SN location and the integrated galaxy flux (Yuan et al. in prep.). We find that SN 2012hn lies at a distance of more than three times the half-light ellipse. The ellipse passing through the SN encloses 88% of its R -band light or 92% of its K -band light (using images from the 2MASS archive). The latter is often used as a proxy for stellar mass.

SN 2012hn represents another example of a peculiar event occurring in the outer regions of an early-type host. Although it is not as distant as some others (e.g. see Kasliwal et al. 2012), the 6.2 kpc is a projected distance, and the deprojected offset will likely be larger. Such an apparent preference for remote locations is different from type Ia and type II SNe that roughly follow the light distribution in their hosts (Förster & Schawinski 2008, Yuan et al. in prep.),

⁴ The European Large Program was a large NTT program (PI S. Benetti) to study nucleosynthesis of SNe. The project ended in September 2012 and shared time with PESSTO during period 89.

⁵ <http://leda.univ-lyon1.fr/>

⁶ From NED, including a correction for Local-Group infall onto the Virgo cluster.

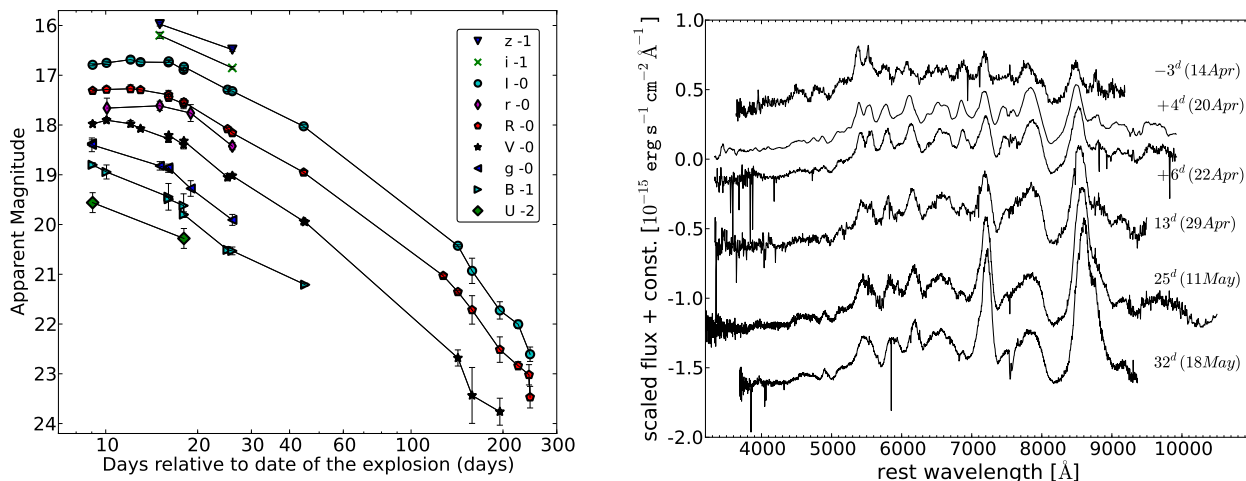


Figure 1. Left: Photometry of SN 2012hn in *UBgVrRiIz*. The date of the explosion has been fixed 12 ± 3 days before *R*-band maximum light ($JD_{\text{exp}} = 2,456,022.5$). Right: Full sequence of photospheric spectra collected for SN 2012hn.

Table 1. Journal of spectroscopic observations. The spectra are available in electronic format on WISeREP (the Weizmann interactive supernova data repository - Yaron & Gal-Yam 2012).

Date	JD -2,400,000	Phase ^a (days)	Range (Å)	Resolution FWHM ^b (Å)	Equipment ^c
2012 Apr 14	56031.52	-3	3800–9200	27	NTT+EFOSC2+Gr13
2012 Apr 20	56038.54	+4	3400–10000	15	NTT+EFOSC2+Gr11/Gr16
2012 Apr 22	56040.49	+6	3400–10000	15	NTT+EFOSC2+Gr11/Gr16
2012 Apr 29	56047.50	+13	3400–10000	15	NTT+EFOSC2+Gr11/Gr16
2012 May 11	56059.48	+25	3000–24000	1,2,8	VLT+XSHOOTER
2012 May 18	56066.49	+32	3700–9000	8	MAG+LDSS3+VPH
2012 Sep 13	56183.87	+149	3000–10000	1	VLT+XSHOOTER
2012 Sep 14	56184.87	+150	3000–10000	1	VLT+XSHOOTER

^a Relative to *R*-band maximum light ($JD = 2,456,034.5$).

^b FWHM of night-sky emission lines.

^c NTT = ESO New Technology Telescope; VLT = ESO Very Large Telescope; MAG = Magellan

and from SNe Ib/c that are more centrally concentrated in galaxies (Kelly, Kirshner & Pahre 2008; Anderson & James 2009; Leloudas et al. 2011).

The remote location of SN 2012hn in the host galaxy is an immediate indirect evidence for low extinction along the line of sight. On the other hand, the observed colours of SN 2012hn are rather extreme. Few (if any) SNe have been observed to be so red, which might therefore suggest at least some extinction. A comparison of the SED with those of objects with similar spectral features is a frequently used method to estimate the reddening. An alternative approach is based on the strength of narrow sodium lines in the spectrum.

Gas and dust are often mixed, and some authors have claimed the existence of a statistical correlation between the EW of Na I D lines and the colour excess (Munari & Zwitter 1997; Turatto, Benetti & Cappellaro 2003). These results have been questioned (Poznanski et al. 2011), but very recently confirmed on the basis of an analysis of a large sam-

ple of Sloan spectra (Poznanski, Prochaska & Bloom 2012). The fact that Na I D is easily saturated makes this method inaccurate for high reddening values, while at low reddening the spread of the relation is very high. In the XSHOOTER spectrum the Na I D doublet is identified at a redshift of 0.0076, 150 km s^{-1} displaced to the red with respect to the systemic velocity ($z = 0.0071$) (Fig. 3). We measured an equivalent width of 0.55 and 1.0 \AA for the D2 and D1 components, respectively. D1 should have twice the intensity of D2. Convolving our XSHOOTER spectrum with a gaussian of 15 \AA (which is typical of our low-resolution spectra) causes the lines to disappear, which confirms that the non-detection in the lower-resolution spectra is not surprising.

Using the relation of Poznanski, Prochaska & Bloom (2012), SN 2012hn will have an $E(B - V)_{\text{NGC 2272}} = 0.2$ mag. This reddening value would make SN 2012hn very similar to the faint type I SNe 2005E (Perets et al. 2010) and 2010et (Kasliwal et al. 2012) in the *R* and *I* bands, while it would remain the faintest object among these three in the

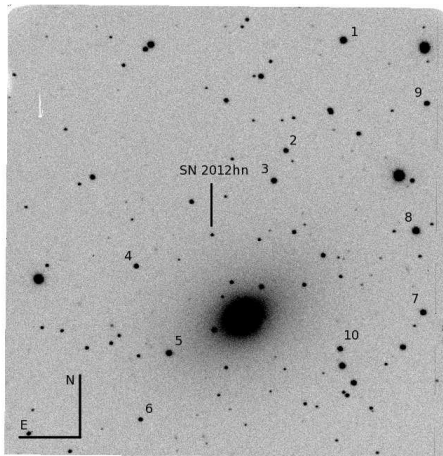


Figure 2. NTT+EFOSC2 R -filter image of the field of SN 2012hn (4×4 arcmin²). The local sequence stars of Tables A3 and A4 are labelled.

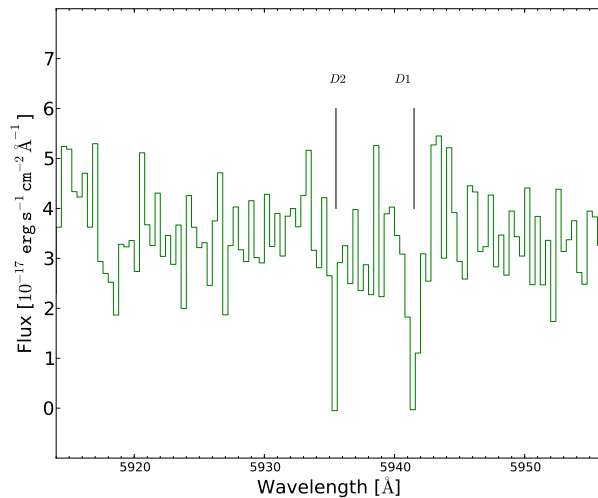


Figure 3. Na I D from the host galaxy.

Table 2. Main parameters for SN 2012hn and its host galaxy.

Parent galaxy	NGC 2272
Galaxy type	E/S0 (LEDA) / SAB0 (NED)
RA (J2000)	06 ^h 42 ^m 42 ^s .55
Dec (J2000)	-27°26′49″.8
Recession velocity ^a	1917 km s ⁻¹
Distance modulus ^b	32.14 ± 0.15 mag
$E(B - V)_{\text{NGC 2272}}$	0.2 mag
$E(B - V)_{\text{MW}}^c$	0.105 mag
Offset from nucleus	18.75 arcsec E, 44.20 arcsec N
Maximum epoch in V (JD)	2456032.5 ± 1.0 (Apr 15, 2012)
Maximum epoch in R (JD)	2456034.5 ± 1.0 (Apr 17, 2012)

^a From LEDA, velocity corrected for Local-Group infall onto the Virgo cluster.

^b From NED, corrected for Local-Group infall onto the Virgo cluster and assuming $H_0 = 72$ km s⁻¹ Mpc⁻¹.

^c Schlegel, Finkbeiner & Davis (1998).

B band (see Fig. 4). In this paper we adopt a colour excess $E(B - V)_{\text{NGC 2272}} = 0.2$ mag for the host of SN 2012hn.

4 LIGHT CURVES

Photometrically, SNe 2005E and 2010et provide the closest matches to SN 2012hn. Among the other faint type I SNe, SN 2005cz (Kawabata et al. 2010) and PTF11bij (Kasliwal et al. 2012) show a similar decline in the R band, but due to poor coverage around maximum the peak luminosity is not well constrained (see Fig. 5a). PTF09dav (Sullivan et al. 2011) has very similar luminosity in the R band, while SN 2007ke is brighter and has a broader light curve than all the other objects of this class. Its connection to the faint type I transient family cannot be safely established.

It has been claimed that Ca-rich SNe show a faster luminosity evolution than other type I SNe. Their light curves likely have a rise time ≤ 15 days (Kasliwal et al. 2012) and they seem to evolve faster than normal SNe Ia and most SNe Ib/c. The rise time of SNe Ia is ~ 18 days (Ganeshalingam, Li & Filippenko 2011; Hayden et al.

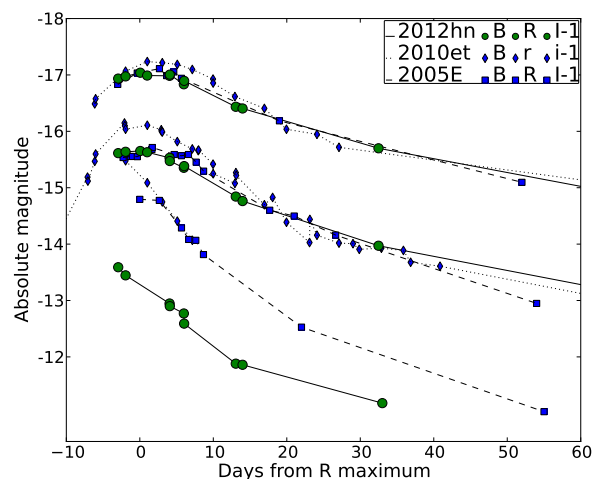


Figure 4. Light-curve comparison of SNe 2005E, 2010et and 2012hn.

2010), while on average SNe Ib have a rise time ≥ 20 days (Valenti et al. 2011). However, SN 1994I, one of the fastest evolving SNe Ic ever studied, has an even faster light curve evolution with a rise time of ~ 11 days (see Fig. 5b).

The colour-curve comparison in Fig. 6 confirms that SN 2012hn is very red, one magnitude redder than the closest matches, SNe 2005E and 2010et. All these SNe show a deficit of flux in the B band and a very fast evolution in the blue bands, suggesting a rapid cooling of the ejecta.

5 SPECTRA

SN 2012hn displays significant peculiarities in its spectral evolution. The deficit of flux in the B band is visible in all the spectra (see Fig. 1). The photospheric velocity, derived from spectral fits with SYNOW (Fisher 2000), is almost con-

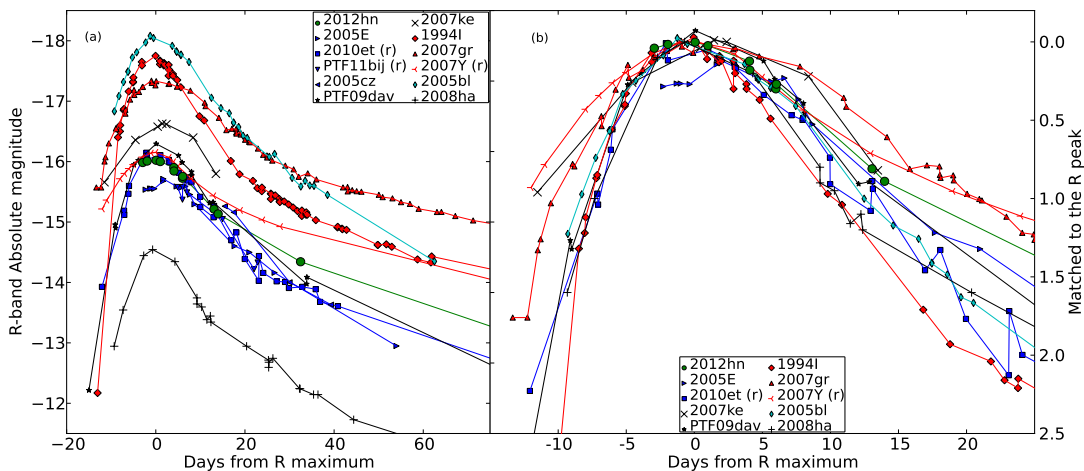


Figure 5. *R*-band photometry of SN 2012hn in comparison with other objects. Data: SN 1994I, Richmond et al. (1996); SN 2005E, Perets et al. (2010); SN 2005bl, Taubenberger et al. (2008); SN 2005cz, Kawabata et al. (2010); SN 2007Y, Stritzinger et al. (2009); SN 2007gr, Valenti et al. (2008b) and Hunter et al. (2009); SN 2007ke, Kasliwal et al. (2012); SN 2008ha, Valenti et al. (2009); PTF09dav, Sullivan et al. (2011); SN 2010et, Kasliwal et al. (2012); PTF11bij, Kasliwal et al. (2012).

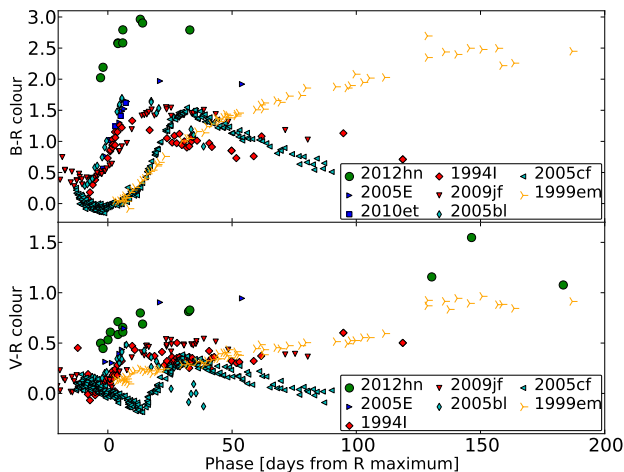


Figure 6. The $B - R$ and $V - R$ colour curves for a sample of supernovae. Data: SN 1999em, Elmhamdi et al. (2003); SN 2005cf, Pastorello et al. (2007b); SN 2009jf, Valenti et al. (2011); see Fig. 5 for other SNe references.

stant with phase. We determine an expansion velocity of $\sim 10000 \text{ km s}^{-1}$, and the spectral lines appear even more blended at late times than at early phases. In addition, while the minima of the absorptions remain at the same positions, the peaks of selected emission features, though still blueshifted, move to redder wavelengths with time. In particular, the emission at $\sim 7195 \text{ \AA}$ (rest frame) shifts by $\sim 35 \text{ \AA}$ in one month (from 7180 \AA on 2012 April 14.02 to 7215 \AA on 2012 May 18.97). This line could be identified with forbidden $[\text{Ca II}] \lambda\lambda 7291, 7323$. Its intensity increases with time (as expected for forbidden lines) and the blueshift goes from 5000 km s^{-1} in the first spectrum to 3500 km s^{-1}

in the last photospheric spectrum, assuming the identification with $[\text{Ca II}] \lambda\lambda 7291, 7323$ is correct. Noticeably, this line is already visible in our first spectrum, taken before maximum light. The unusual velocity evolution in SN 2012hn is difficult to explain. Normally, absorption lines in SNe tend to become narrower with time, as the outer layers become more diluted by the expansion of the ejecta and the line-forming region recedes to lower velocities. In SN 2012hn we observe the opposite trend: constant photospheric velocity (as inferred from the blueshift of absorption lines) and increasing line widths.

5.1 Spectra of faint type I SNe

In Fig. 7, we show a set of spectra that includes several faint type I objects (SNe 2005E, 2005cz and 2010et) and the peculiar PTF09dav. SNe 2005E and 2010et appear to be very similar, except for the intense peak at $\sim 4500 \text{ \AA}$ visible in SN 2005E. He I is detected in both of them and strong Ca II lines appear later on. On the other hand there are several differences with the spectra of PTF09dav as already pointed out by Kasliwal et al. (2012). In particular the lack of He I features and the presence of Sc II lines make PTF09dav an outlier. We note that He I is absent also in the spectra of SN 2012hn, and we do not see any evidence for the presence of Sc II lines. The spectra of SN 2012hn are also quite different from the spectra of SNe 2005E and 2010et (see Fig. 7). This implies a high degree of heterogeneity in the spectra of faint type I objects, raising the possibility that not all of these objects come from the same progenitor systems or share the same explosion mechanism.

As previously mentioned, at the classification stage, we did not find objects in any of the publicly available archives with a spectrum similar to that of SN 2012hn, and we were unable to identify all the spectral lines. In principle, the lack of strong H and He I lines would favour the classification as a peculiar SN Ic. Indeed,

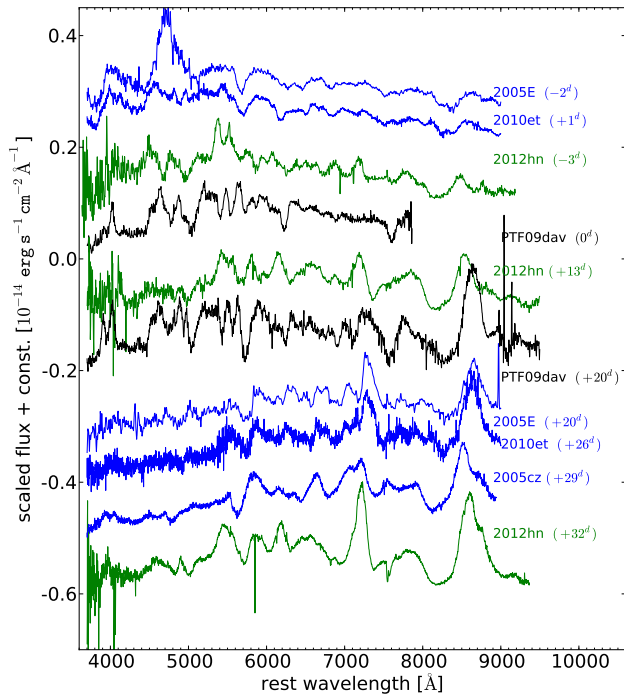


Figure 7. Spectra comparison of SNe that have been suggested as Ca-rich. See Fig. 5 for references.

the comparison with a library of supernova spectra via GELATO (Harutyunyan et al. 2008) shows a best match with SN 1990aa (Filippenko, Shields & Petschek 1990) and several other SNe Ic.

In Fig. 8a we compare SN 2012hn with SN 1990aa (Matheson et al. 2001). The spectrum of SN 2012hn shows in parts the same features as SN 1990aa, although some emission features are much stronger in the former. The main differences are the strong emissions at ~ 6100 Å, ~ 7200 Å and ~ 8700 Å. Around 7500 Å SN 1990aa shows O I $\lambda 7774$, which is not visible in SN 2012hn. In this region, at earlier phases, SN 2012hn shows two absorption features, redward and blueward respectively of the expected position of O I $\lambda 7774$.

In the case of SN 2005E, the most similar object was identified in SN 1990U (Perets et al. 2010). A comparison is shown in Fig. 8b. Both SN 2005E and SN 1990U show clear He I $\lambda 5876$, $\lambda 6678$ and $\lambda 7065$ lines. It is interesting to point out that both SN 2012hn and SN 2005E are similar to quite normal SNe Ic and SNe Ib, respectively, though with more prominent Ca features.

Given these similarities, it is tempting to propose that faint type I SNe arise from similar progenitors as SNe Ib/c, though with an overproduction of Ca in the explosive nucleosynthesis or with ionisation and excitation conditions in the ejecta that favour the formation of strong Ca II features.

Starting from the similarity with SN 1990aa, we used SYNOW to identify the lines in the SN 2012hn spectra. Fits to the spectra collected on April 20th (+4 days) and May 18th (+32 days) are shown in Figs. 9a and 9b, respectively. A photospheric velocity of 10000 km s^{-1} was adopted in both cases, while we used temperatures of 4500 K for the

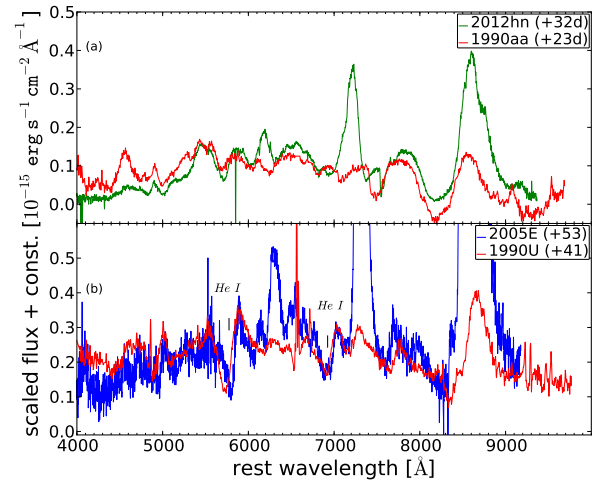


Figure 8. Comparison of SN 2012hn and SN 2005E with SN 1990aa and SN 1990U, respectively. The latter have been identified as best spectroscopic matches to the former. Data are from Matheson et al. (2001) and Filippenko (1992).

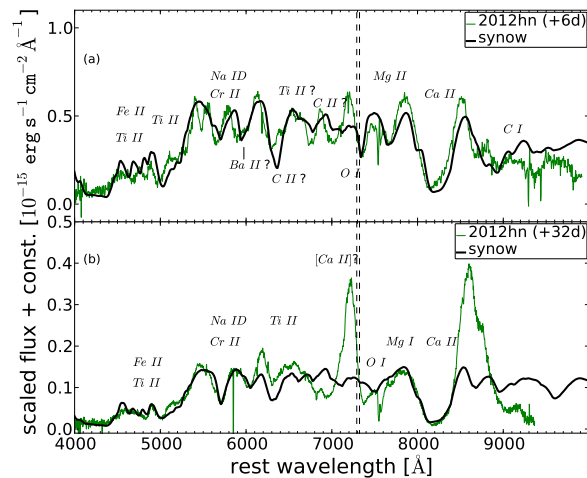


Figure 9. SYNOW fit of SN 2012hn spectra. The dashed lines indicate the rest-frame positions of $[\text{Ca II}] \lambda\lambda 7291, 7323$.

spectrum at +6 days and 4200 K for the spectrum at +32 days. The radial dependence of the line optical depths was chosen to be exponential with the e -folding velocity v_e [i.e. $\tau \propto \exp(-v/v_e)$] set to 1000 km s^{-1} for both spectra. The spectra can be reproduced reasonably well with a small number of ions, including Fe II, Ca II, C I, Cr II, Ti II and Na I. Most lines between 6000 and 7500 Å can be reproduced by enhancing Fe II and Ti II. The line at ~ 5800 Å may be reproduced by Na I and Cr II or detached He I, but we consider the He I identification unlikely because of the lack of other He I lines both in the optical and the NIR regime (see Sec. 5.2). Some Fe II lines may also contribute to this feature. Mg II is an alternative for the absorption at 7700 Å, redward of the usual O I position. The absorption at ~ 7350 Å, blueward of the usual O I position may still be explained with O I. We

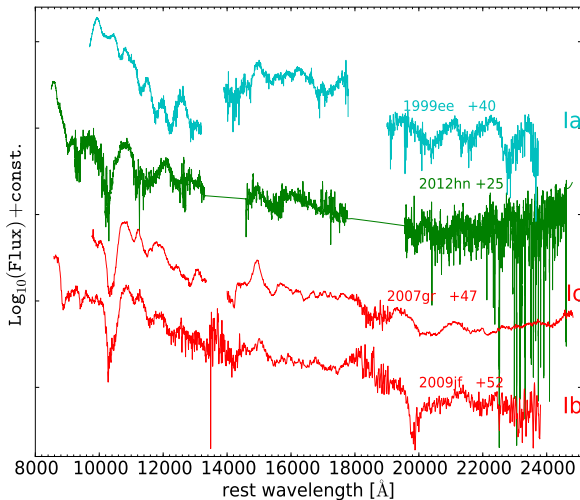


Figure 10. XSHOOTER NIR spectrum of SN 2012hn in comparison with spectra of other SNe. The SN 2012hn spectrum has been rebinned to 20 Å bins. Comparison spectra are from Hamuy et al. (2002); Hunter et al. (2009); Sahu et al. (2011).

stress that intermediate-mass elements such as Si and S are not required to reproduce the spectrum of SN 2012hn. In the first spectrum including some Ba II may help to reproduce the feature at 5900 Å. The presence of Ba II, if confirmed, would be important, since Ba II is not expected in thermonuclear explosions. Unfortunately, we consider this identification not as secure as other identifications, since it is mainly based on a single line.

The main shortcomings of the synthetic spectrum are the emission features at ~ 7200 Å and ~ 8700 Å which are not reproduced. If the former (~ 7200 Å) is identified as blueshifted [Ca II] or [O I], the poor fit is not surprising, since SYNOW can not reproduce forbidden lines.

5.2 SN 2012hn NIR spectrum

The XSHOOTER spectrum of SN 2012hn collected on 2012 May 11.98 for the first time gives us the possibility to probe the NIR spectrum of a faint type I SN (see Fig. 10). The red part of the spectrum is quite noisy, but still it can be used to exclude the presence of a strong He feature at ~ 2 micron, which is typical of He-rich SNe. Normal SNe Ia show intense lines of Co II and Fe II at this phase (Marion et al. 2009; Gall et al. 2012). These lines are not expected in SN 2012hn because of the low observed luminosity and hence small amount of ^{56}Ni synthesized in the explosion. The XSHOOTER spectrum also gives us information on the amount of flux emitted in the NIR. After checking the XSHOOTER spectrum flux calibration with our optical photometry, we computed a synthetic $R - H$ colour (~ -0.5 to 0.0 mag). This value is comparable with the $R - H$ colour of several SNe Ia (Krisciunas et al. 2004), and much lower than the $R - H$ colour of core-collapse SNe at this phase ($R - H \sim 1$ mag).

5.3 Late-time spectroscopy

Two XSHOOTER spectra were obtained 149 and 150 days after R -band maximum, and the combination of their optical parts is compared with nebular spectra of different types of SNe in Fig. 11. No flux has been detected in the NIR part of the combined XSHOOTER spectrum down to a mag of ~ 22.5 in the H band.

The emission centred at ~ 7250 Å is most likely [Ca II] $\lambda\lambda 7291, 7323$, with a contribution of [Fe II] to the blue ($\lambda\lambda 7155, 7172$) and the red ($\lambda\lambda 7388, 7452$) wings. Mg I $\lambda 4571$ is also detected. No permitted lines of O I ($\lambda 7774$ or $\lambda 8446$) are visible, and also the Ca NIR triplet, very strong at early phases, has faded. An emission feature at ~ 8700 Å is likely a blend of residual, weak Ca II and [C I] $\lambda 8727$. The absence of permitted lines gives us a constraint on the density, confirming that the spectrum is nebular (Fransson & Chevalier 1989). Comparing SN 2012hn with other faint type I SNe, the weakness of the Ca II NIR triplet is not unusual. However, the prominent [O I] $\lambda\lambda 6300, 6364$ feature is quite unique among faint type I SNe. It is much more similar in terms of relative strength to spectra of stripped core-collapse SNe, which show strong [O I] owing to oxygen produced in the progenitor star. The feature is symmetric around the rest wavelength and relatively narrow, with emission out to 3500 km s^{-1} .

We computed the [Ca II]/[O I] ratio for a large set of nebular spectra of core-collapse SNe and the sample of faint type I SNe presented by Kasliwal et al. (2012) (see Fig. 12). For almost all core-collapse SNe [Ca II] $\lambda\lambda 7291, 7323$ starts to be visible earlier than [O I] $\lambda\lambda 6300, 6364$, but rarely less than 100 days after maximum light. Faint type I SNe show both these lines earlier on, but no data are available later than 170 days after maximum to study the intensity evolution of these features over longer time scales. Fig. 12 confirms that the [Ca II]/[O I] ratio of SN 2012hn is at the edge of the region occupied by core-collapse SNe.

6 BOLOMETRIC LIGHT CURVE

To constrain the physical parameters of SN 2012hn (M_{Ni} , M_{ej} and E_{k}), we computed a pseudo-bolometric light curve using the available photometric information. As long as the light curve is powered by the $^{56}\text{Ni} \rightarrow ^{56}\text{Co} \rightarrow ^{56}\text{Fe}$ decay chain, a brighter bolometric light curve implies a larger amount of ejected ^{56}Ni . In addition, the broader the light curve, the higher the ejected mass and/or the lower the kinetic energy released in the explosion (Arnett 1982).

To compute the pseudo-bolometric light curve, the flux was integrated from the U to the I band assuming $E(B - V)_{\text{NGC } 2272} = 0.2$ mag and $\mu = 32.14$ mag. The so-created pseudo-bolometric light curve is plotted in Fig. 13 together with those of other SNe computed following the same prescriptions. In core collapse SNe the NIR flux contributes up to 40–50 % to the total flux, in SNe Ia up to 30 % (Valenti et al. 2008a). Given the $R - H$ colour measured from our first XSHOOTER spectrum, we assumed that the fractional contributions of the UV and NIR emission to the bolometric light curve of SN 2012hn are the same as for the type Ia SN 2005cf (Pastorello et al. 2007b) With this assumption, we computed a *voir* pseudo-bolometric light curve of SN 2012hn, which is also shown in Fig. 13.

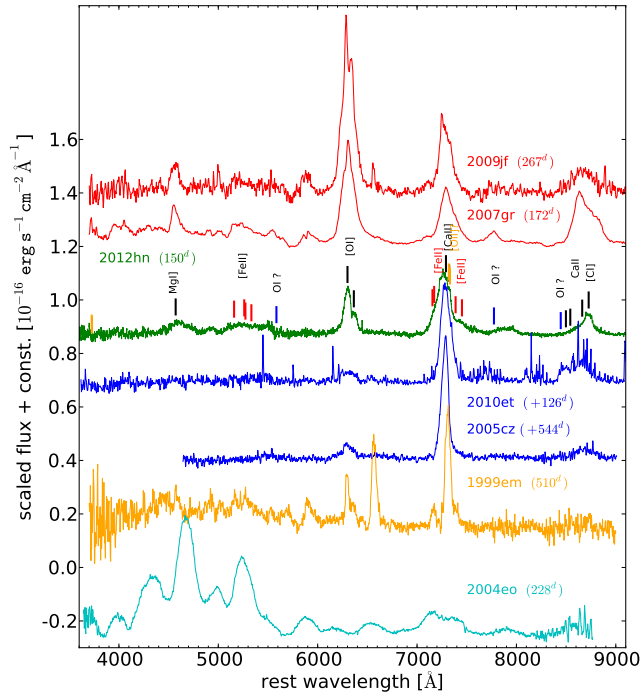


Figure 11. Nebular spectrum of SN 2012hn in comparison with a set of nebular spectra of different types of SNe. Tentative line identifications are given for the spectrum of SN 2012hn. Data: SN 2009jf, Valenti et al. (2011); SN 2007gr, Hunter et al. (2009); SN 2010et, Kasliwal et al. (2012); SN 2005cz, Kawabata et al. (2010); SN 1999em, Elmhamdi et al. (2003); SN 2004eo, Pastorello et al. (2007a).

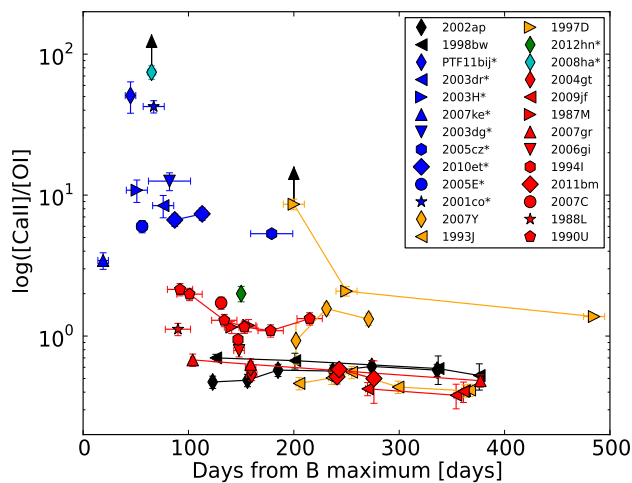


Figure 12. The $[\text{CaII}]/[\text{OI}]$ ratio as a function of time for a sample of SNe. For objects labelled with * the phase is given relative to R -band maximum or relative to discovery. Data from Taubenberger et al. (2009, and references therein), Valenti et al. (2009), Hunter et al. (2009), Stritzinger et al. (2009), Valenti et al. (2011), Valenti et al. (2012), Kasliwal et al. (2012), Turatto et al. (1998).

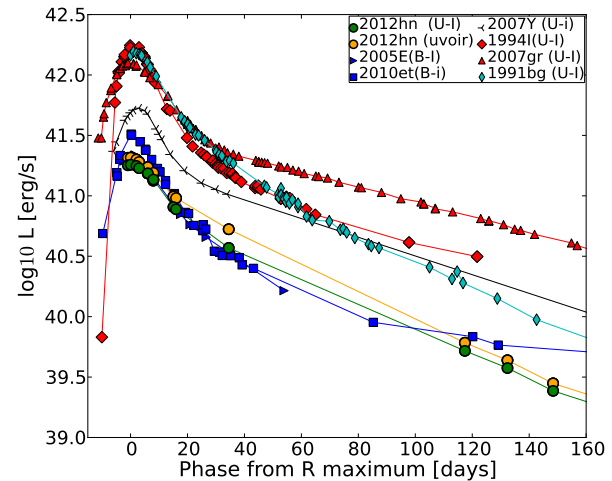


Figure 13. Pseudo-Bolometric light curve of SN 2012hn in comparison with other SNe. Data: see references in Fig. 5; SN1991bg, Turatto et al. (1996). Distances and colour excesses: - SN 1994I: $E(B - V) = 0.04$ mag, $\mu = 29.60$ mag, (Sauer et al. 2006); - SN 2007gr: $E(B - V) = 0.092$ mag, $\mu = 29.84$ mag, (Valenti et al. 2008b); - SN 2007Y: $E(B - V) = 0.112$ mag, $\mu = 31.13$ mag, (Stritzinger et al. 2009); - SN 2005E: $E(B - V) = 0.041$ mag, $\mu = 32.66$ mag, (Perets et al. 2010); - SN 2010et: $E(B - V) = 0.046$ mag, $\mu = 35.05$ mag, (Kasliwal et al. 2012); - SN 1991bg: $E(B - V) = 0.029$ mag, $\mu = 31.44$ mag, (Turatto et al. 1996).

The lack of data before maximum and hence the unknown rise time of SN 2012hn makes it difficult to derive accurate explosion parameters. A rough estimate of M_{ej} and E_{k} can be computed guided by the comparison with well-studied SNe and the following simple relations: $v \propto (E_{\text{k}}/M_{\text{ej}})^{1/2}$ and $t_{\text{s}} \propto (M_{\text{ej}}^3/E_{\text{k}})^{1/4}$, where v is the photospheric velocity (evaluated at maximum light) and t_{s} is the time scale of the photospheric phase (Arnett 1982). Using a Chandrasekhar-mass SN Ia as comparison ($E_{\text{k}} = 1.3 \times 10^{51}$ erg, $M_{\text{ej}} = 1.4 M_{\odot}$, $v = 10000 \text{ km s}^{-1}$, the photospheric velocity of SN 2012hn ($v = 10000 \text{ km s}^{-1}$) and a time scale of t_{s} (SN 2012hn) = $0.7-0.8 t_{\text{s}}$ (SNe Ia) (from light-curve comparisons), we obtain the following values for SN 2012hn: $M_{\text{ej}} = 0.7-0.9 M_{\odot}$ and $E_{\text{k}} = 0.65-0.85 \times 10^{51}$ erg. Using instead the type Ib SN 2008D as reference, adopting the values of M_{ej} and E_{k} reported by Tanaka et al. (2009), we obtain estimates three times as large for the energy and the ejected mass ($M_{\text{ej}} = 1.9-2.6 M_{\odot}$ and $E_{\text{k}} = 2.2-4.1 \times 10^{51}$ erg). Perets et al. (2010), using the same approach, obtained much smaller values for SN 2005E ($M_{\text{ej}} = 0.25-0.41 M_{\odot}$ and $E_{\text{k}} = 0.44-0.72 \times 10^{51}$ erg). This is because they adopted a very short rise time of 7–9 days. Actually we argue that from the light-curve comparison with SN 1994I (with a rise time of 11 days) (see Fig. 4), a rise time of 7–9 days for SN 2005E is probably an underestimate. From the similarity of the light curves of SNe 1994I, 2005E and 2012hn, and given the fact that they have similar photospheric velocities, using the simple relations reported above we would expect similar values for the ejected masses and kinetic energies. The different values obtained mainly reflect our uncertainties in some of the important fitting constraints, such as the rise time.

From the absolute luminosity of SN 2012hn, if the light

curve is powered by nickel decay, the mass of ^{56}Ni produced in the explosion should be $M_{\text{Ni}} = 0.005\text{--}0.010 M_{\odot}$ assuming a rise time between 10 and 15 days. However, as pointed out by several authors, in low-density explosions decays of radioactive nuclei other than ^{56}Ni may be important (Shen et al. 2010; Waldman et al. 2011; Sim et al. 2012). In particular the decays $^{48}\text{Cr} \rightarrow ^{48}\text{V} \rightarrow ^{48}\text{Ti}$ and $^{44}\text{Ti} \rightarrow ^{44}\text{Sc} \rightarrow ^{44}\text{Ca}$ may play an important role in powering the light curve (the latter only at late phases). The nickel mass produced may hence be even lower than the one reported. Ti and Cr may also be responsible for the fast evolution in the blue bands and the relatively red colour by depressing most of the flux in the blue part of the spectrum. The slope of the bolometric light curve in the tail phase is comparable to that of the type Ia SN 1991bg and faster than in most other SNe. SN 2010et, the only Ca-rich SN with multi-band late-time photometry, shows a similar slope until 80 days after *R*-band maximum. After this point, the bolometric light curve of SN 2010et is contaminated by the flux from its host galaxy (Kasliwal et al. 2012). The steady slope of the tail of SN 2012hn suggests that a single decay is powering the light curve at these phases.

7 DISCUSSION AND CONCLUSIONS

SN 2012hn belongs to the class of faint type I SNe, showing a light curve that is very similar to those of SNe 2005E and 2010et. It has a low peak luminosity and evolves rapidly (although not as fast as SN 1994I). Faint type I transients show heterogeneous spectral properties. In particular, SN 2012hn shows no clear evidence of He I features, and the early-time spectra resemble those of a SN Ic with superimposed forbidden lines of Ca II. Contrary to what we typically see in SNe, line widths tend to increase with time, while the photospheric velocity remains almost constant at $\sim 10000 \text{ km s}^{-1}$ during the entire photospheric phase.

One of the most intriguing features is the presence, very early on, of a strong emission feature at about 7200 \AA . Based on the very strong Ca II NIR triplet and the lack of viable alternatives, we attribute this feature to forbidden Ca II. However, if this is correct, the peak of the emission is blueshifted by $3000\text{--}5000 \text{ km s}^{-1}$ with respect to the rest-frame position. Since the blueshift decreases with time, it is unlikely due to dust forming and may be explained by an optically thick core of the ejecta (Taubenberger et al. 2009) or by strong asymmetry in the explosion. On the other hand, the [O I] profile in the nebular spectrum is consistent with a spherically symmetric distribution of the ejecta, or at least of the oxygen-rich material.

In the last few years several studies have been carried out to explain faint type I transients. Most of them have focused on He-shell detonations on accreting carbon-oxygen white dwarfs (WDs) (Bildsten et al. 2007; Shen et al. 2010; Waldman et al. 2011; Sim et al. 2012).

In the double-detonation scenario for SNe Ia, the He-shell detonation is followed by a second detonation in the core of the carbon-oxygen WD. While it is still not clear if and where the second detonation occurs (but see Fink, Hillebrandt & Röpke 2007; Fink et al. 2010), a pure He-shell detonation might produce an explosion with several characteristics similar to the explosion of SN 2012hn.

Shen et al. (2010) investigated He-shell detonations for three different WD masses ($0.6, 1.0, 1.2 M_{\odot}$) and different He-shell masses ($0.02, 0.05, 0.1, 0.2, 0.3 M_{\odot}$). Waldman et al. (2011) focused their study on low-mass WDs ($0.45\text{--}0.6 M_{\odot}$) with a $0.2 M_{\odot}$ He shell. Also Sim et al. (2012) studied He-shell detonations on low-mass WDs ($0.45\text{--}0.58 M_{\odot}$) with a $0.21 M_{\odot}$ He shell, but extended the simulations to cases where a second detonation occurs. These studies tend to find that the amount of intermediate-mass elements (Si, S) produced during the explosion is lower than in *normal* SNe Ia whereas Ti and Cr are produced abundantly. The resultant spectrum is also rich of Ti and Cr lines. While this is consistent with the spectra of SN 2012hn, the light curve may be different. If the second detonation occurs, the models show light curves brighter than that of SN 2012hn (Sim et al. 2012). If the second detonation does not occur, the peak luminosity is comparable, but the evolution is much faster than that of SN 2012hn. Waldman et al. (2011) were able to obtain a light curve comparable to SN 2005E for their He-shell detonation model WD ($0.45 M_{\odot}$) + He-shell ($0.2 M_{\odot}$), but only with an artificial ^{44}Ti enhancement by a factor of 50. All the He-shell detonation models in low-mass WDs predict red spectra with Ti lines and no intermediate-mass elements, but none of them predict the slow spectral evolution of SN 2012hn. So far, no synthetic nebular spectra of He detonations on accreting WDs have been made. Unburned C/O can be present in a He-shell detonation if the second detonation in the WD does not occur. The He-shell detonation model of Sim et al. (2012) shows oxygen below 4000 km s^{-1} , consistent with the oxygen velocity in the nebular spectrum of SN 2012hn. Whether this amount of oxygen is enough and the density and ionisation in the innermost ejecta are suited to produce the observed nebular oxygen line of SN 2012hn is still not clear. An estimate of the ejected mass of oxygen and carbon from the nebular SN 2012hn spectrum would be the next step in this analysis (Mazzali et al. 2007, 2010).

Little Si and S, the presence of Ti and Cr, and [OI] in the nebular spectrum are also expected in core-collapse SNe. Nevertheless, only few theoretical studies have been made so far to explain faint type I SNe as core-collapse explosions. Kawabata et al. (2010) proposed for SN 2005cz a progenitor of $8\text{--}12 M_{\odot}$ that lost its envelope through interaction in a binary system. These stars are more abundant than more massive stars, and some of them should still be present in E/S0 galaxies. If the hydrogen layer has been stripped by a companion star, they might still produce core-collapse SNe similar to SNe Ib and Ic. As stripped-envelope counterparts of faint type IIP SNe (Pastorello et al. 2004), a population of faint SNe Ib/c may be expected to exist. These objects have not been unambiguously identified in observations so far (but see Valenti et al. 2009), but faint type I SNe could be viable candidates. The weak point of this interpretation is that, so far, no faint type IIP SNe have been discovered in remote locations of E/S0 galaxies. Detailed models for faint stripped-envelope core-collapse SNe are missing, and again a detailed model of this explosion scenario would be the next step to constrain their physical properties.

In summary, the physical origin of this faint type I SN 2012hn is still ambiguous. The location of the transient, in the remote outskirts of an E/S0 type galaxy indicates an origin in an old stellar population and hence an accreting WD system as the most likely progenitor. The lack of

any possible dwarf host galaxy to quite faint magnitudes in pre-discovery images (to below about $M = -11$) argues either for a non-star-forming population or an ultra-faint dwarf galaxy with presumably low metallicity. However, the nebular spectrum of SN 2012hn at +150d shows the strongest oxygen feature yet detected among faint type I SNe, similar in strength to [O I] seen in core-collapse SNe. Mg I and C I features are also detected, which are weak or not detected in other faint type I SNe, but usually seen in core-collapse events.

Among the other faint type I SNe discovered so far, SNe 2010et and 2005E have similar light curves and are in even more remote locations with respect to their hosts. This appears to be a strong argument in favour of the WD as progenitors. However, if a single scenario gives rise to these events, it must be able to reproduce the differences in their spectra, in particular the small amount of helium (if any) in SN 2012hn and the differences already mentioned in the nebular spectra, and to produce an ejected mass in the range (~ 0.5 – $1.5 M_{\odot}$), comparable with the ejected masses of low-mass, low-energy SNe Ib/c. Detailed modelling of the nebular spectra of this class may help to further constrain the origins of these peculiar and intriguing explosions (e.g. Mazzali et al. 2010, 2011; Maurer et al. 2011; Jerkstrand et al. 2012) and to confirm or disprove the large Ca abundance reported for SN 2005E by Perets et al. (2010).

Including other faint transients, such as PTF09dav or SN 2008ha, in the same scenario will be even more complicated, emphasizing the possibility that faint type I SNe may actually arise from several different explosion channels.

ACKNOWLEDGEMENTS

G.P. acknowledges support by the Proyecto FONDECYT 11090421. J. A. acknowledges support by CONICYT through FONDECYT grant 3110142. G.P. and J.A. acknowledge support by the Millennium Center for Supernova Science (P10-064-F), with input from Fondo de Innovación para la Competitividad, del Ministerio de Economía, Fomento y Turismo de Chile. S.T. acknowledges support by the TRR 33 ‘The Dark Universe’ of the German Research Foundation. MS acknowledges support from the Royal Society. This work was supported by the National Science Foundation under grants PHY 11-25915 and AST 11-09174. Research leading to these results has received funding from the European Research Council under the European Union’s Seventh Framework Programme (FP7/2007-2013)/ERC Grant agreement n° [291222] (PI : S. J. Smartt). A.P. S.B. and E.C. are partially supported by the PRIN-INAF 2011 with the project ‘‘Transient Universe: from ESO Large to PESSTO’’. Research by AGY and his group is supported by the FP7/ERC, Minerva and GIF grants. Parts of this research were conducted by the Australian Research Council Centre of Excellence for All-sky Astrophysics (CAASTRO), through project number CE110001020. We are grateful to Douglas Leonard who provided us his spectrum of SN 2005cz.

This paper is based on observations made with the following facilities: ESO Telescopes at the La Silla and Paranal Observatories under programme IDs 184.D-1140,

188.D-3003, 089.D-0270, Prompt telescopes (Chile). Trappist telescope (Chile), Du Pont telescope (Chile), Magellan telescope (Chile). Observations under programme ID 188.D-3003 are part of PESSTO (the Public ESO Spectroscopic Survey for Transient Objects). The spectra of Kasliwal et al. (2012) were downloaded from WISEREP (Yaron & Gal-Yam 2012).

REFERENCES

- Anderson J. P., James P. A., 2009, Monthly Notices of the Royal Astronomical Society, 399, 559
 Arnett W. D., 1982, Astrophysical Journal, 253, 785
 Benitez-Herrera S., Taubenberger S., Valenti S., Benetti S., Pastorello A., 2012, The Astronomer’s Telegram, 4047, 1
 Bildsten L., Shen K. J., Weinberg N. N., Nelemans G., 2007, The Astrophysical Journal, 662, L95
 Drake A. J. et al., 2010, Central Bureau Electronic Telegrams, 2339, 1
 Elmhamdi A. et al., 2003, Monthly Notice of the Royal Astronomical Society, 338, 939
 Filippenko A. V., 1992, Astrophysical Journal, 384, L37
 Filippenko A. V., Chornock R., Swift B., Modjaz M., Simcoe R., Rauch M., 2003, IAU Circ., 8159, 2
 Filippenko A. V., Shields J. C., Petschek A. G., 1990, IAU Circ., 5111, 1
 Filippenko A. V., Silverman J. M., Foley R. J., Modjaz M., Papovich C., Willmer C. N. A., Blondin S., Brown W., 2007, Central Bureau Electronic Telegrams, 1101, 1
 Fink M., Hillebrandt W., Röpke F. K., 2007, Astronomy and Astrophysics, 476, 1133
 Fink M., Röpke F. K., Hillebrandt W., Seitenzahl I. R., Sim S. A., Kromer M., 2010, Astronomy and Astrophysics, 514, 53
 Foley R. J. et al., 2012, arXiv.org, astro-ph.SR, 2209
 Foley R. J. et al., 2009, The Astronomical Journal, 138, 376
 Förster F., Schawinski K., 2008, Monthly Notices of the Royal Astronomical Society: Letters, 388, L74
 Fransson C., Chevalier R. A., 1989, Astrophysical Journal, 343, 323
 Gall E. E. E., Taubenberger S., Kromer M., Sim S. A., Benetti S., Blanc G., Elias-Rosa N., Hillebrandt W., 2012, arXiv.org, 1208, 5949
 Ganeshalingam M., Li W., Filippenko A. V., 2011, Monthly Notices of the Royal Astronomical Society, 416, 2607
 Hamuy M. et al., 2002, The Astronomical Journal, 124, 417
 Harutyunyan A. H. et al., 2008, Astronomy and Astrophysics, 488, 383
 Hayden B. T. et al., 2010, The Astrophysical Journal, 712, 350
 Hunter D. J. et al., 2009, Astronomy and Astrophysics, 508, 371
 Jerkstrand A., Fransson C., Maguire K., Smartt S., Ergon M., Spyromilio J., 2012, Astronomy and Astrophysics, 546, 28
 Kasliwal M. M. et al., 2012, The Astrophysical Journal, 755, 161
 Kasliwal M. M. et al., 2010, The Astrophysical Journal Letters, 723, L98
 Kawabata K. S. et al., 2010, Nature, 465, 326

- Kelly P. L., Kirshner R. P., Pahre M., 2008, *The Astrophysical Journal*, 687, 1201
- Krisciunas K. et al., 2004, *The Astronomical Journal*, 128, 3034
- Leloudas G. et al, 2011, *Astronomy and Astrophysics*, 530, 95
- Marion G. H., Höflich P., Gerardy C. L., Vacca W. D., Wheeler J. C., Robinson E. L., 2009, *The Astronomical Journal*, 138, 727
- Matheson T., Filippenko A. V., Li W., Leonard D. C., Shields J. C., 2001, *The Astronomical Journal*, 121, 1648
- Maurer I., Jerkstrand A., Mazzali P. A., Taubenberger S., Hachinger S., Kromer M., Sim S., Hillebrandt W., 2011, *Monthly Notices of the Royal Astronomical Society*, 418, 1517
- Mazzali P. A. et al., 2007, *The Astrophysical Journal*, 670, 592
- Mazzali P. A., Maurer I., Stritzinger M., Taubenberger S., Benetti S., Hachinger S., 2011, *Monthly Notices of the Royal Astronomical Society*, 416, 881
- Mazzali P. A., Maurer I., Valenti S., Kotak R., Hunter D., 2010, *Monthly Notices of the Royal Astronomical Society*, 408, 87
- Munari U., Zwitter T., 1997, *Astronomy and Astrophysics*, 318, 269
- Pastorello A. et al., 2007a, *Monthly Notices of the Royal Astronomical Society*, 377, 1531
- Pastorello A. et al., 2007b, *Monthly Notices of the Royal Astronomical Society*, 376, 1301
- Pastorello A. et al., 2004, *Monthly Notices of the Royal Astronomical Society*, 347, 74
- Perets H. B. et al., 2010, *Nature*, 465, 322
- Poznanski D. et al., 2010, *Science*, 327, 58
- Poznanski D., Ganeshalingam M., Silverman J. M., Filippenko A. V., 2011, *Monthly Notices of the Royal Astronomical Society: Letters*, 415, L81
- Poznanski D., Prochaska J. X., Bloom J. S., 2012, *Monthly Notices of the Royal Astronomical Society*, 426, 1465
- Rau A. et al., 2009, *Publications of the Astronomical Society of the Pacific*, 121, 1334
- Reichart D. et al., 2005, *Il Nuovo Cimento C*, 28, 767
- Richmond M. W. et al., 1996, *Astronomical Journal* v.111, 111, 327
- Sahu D. K., Gurugubelli U. K., Anupama G. C., Nomoto K., 2011, *Monthly Notices of the Royal Astronomical Society*, 413, 2583
- Sauer D. N., Mazzali P. A., Deng J., Valenti S., Nomoto K., Filippenko A. V., 2006, *Monthly Notices of the Royal Astronomical Society*, 369, 1939
- Schlegel D. J., Finkbeiner D. P., Davis M., 1998, *Astrophysical Journal* v.500, 500, 525
- Shen K. J., Kasen D., Weinberg N. N., Bildsten L., Scannapieco E., 2010, *The Astrophysical Journal*, 715, 767
- Sim S. A., Fink M., Kromer M., Röpke F. K., Ruiter A. J., Hillebrandt W., 2012, *Monthly Notices of the Royal Astronomical Society*, 420, 3003
- Stritzinger M. et al., 2009, *The Astrophysical Journal*, 696, 713
- Sullivan M. et al., 2011, *The Astrophysical Journal*, 732, 118
- Tanaka M. et al., 2009, *The Astrophysical Journal*, 700, 1680
- Taubenberger S. et al., 2008, *Monthly Notices of the Royal Astronomical Society*, 385, 75
- Taubenberger S. et al., 2009, *Monthly Notices of the Royal Astronomical Society*, 397, 677
- Turatto M., Benetti S., Cappellaro E., 2003, in *From Twilight to Highlight: The Physics of Supernovae: Proceedings of the ESO/MPA/MPE Workshop Held at Garching*, INAF, Osservatorio Astronomico di Padova, Vicolo dell'Osservatorio 5, 35122 Padova, Italia, p. 200
- Turatto M., Benetti S., Cappellaro E., Danziger I. J., Della Valle M., Gouiffes C., Mazzali P. A., Patat F., 1996, *Monthly Notices of the Royal Astronomical Society*, 283, 1
- Turatto M. et al., 1998, *Astrophysical Journal Letters* v.498, 498, L129
- Valenti S. et al., 2008a, *Monthly Notices of the Royal Astronomical Society*, 383, 1485
- Valenti S. et al., 2008b, *The Astrophysical Journal*, 673, L155
- Valenti S. et al., 2011, *Monthly Notices of the Royal Astronomical Society*, 416, 3138
- Valenti S. et al., 2009, *Nature*, 459, 674
- Valenti S. et al., 2012, *The Astrophysical Journal Letters*, 749, L28
- Waldman R., Sauer D., Livne E., Perets H., Glasner A., Mazzali P., Truran J. W., Gal-Yam A., 2011, *The Astrophysical Journal*, 738, 21
- Yaron O., Gal-Yam A., 2012, *Publications of the Astronomical Society of the Pacific*, 124, 668

APPENDIX A: TABLES

Table A1. Optical photometry of SN 2012hn (Vega magnitudes in Landolt system)^a.

Date	JD − 2,400,000	Phase ^b	<i>U</i>	<i>B</i>	<i>V</i>	<i>R</i>	<i>I</i>	Source ^c
2012-04-13	56031.56	−2.9	21.561 (200)	19.800 (042)	17.980 (050)	17.310 (027)	16.790 (020)	NTT
2012-04-15	56032.56	−1.9	...	19.944 (141)	17.903 (054)	17.286 (066)	16.751 (032)	PROMPT 5
2012-04-17	56034.56	0.0	17.975 (065)	17.272 (079)	16.686 (053)	PROMPT 5
2012-04-18	56035.50	1.0	18.074 (039)	17.294 (047)	16.736 (047)	PROMPT 5
2012-04-21	56038.55	4.0	...	20.443 (268)	18.277 (073)	17.393 (089)	16.741 (051)	PROMPT 5
2012-04-20	56038.58	4.1	...	20.490 (037)	18.206 (027)	17.450 (021)	16.720 (018)	NTT
2012-04-22	56040.49	6.0	...	20.620 (237)	18.397 (083)	17.570 (102)	16.891 (053)	PROMPT 5
2012-04-23	56040.53	6.0	22.282 (200)	20.800 (054)	18.320 (030)	17.540 (025)	16.830 (031)	NTT
2012-04-29	56047.56	13.1	...	21.510 (064)	19.050 (072)	18.080 (027)	17.290 (036)	NTT
2012-04-30	56048.48	14.0	...	21.530 (078)	19.020 (050)	18.160 (043)	17.320 (039)	NTT
2012-05-19	56066.98	32.5	19.936 (045)	18.952 (039)	...	TRAPPIST
2012-05-19	56066.98	32.5	18.026 (031)	PROMPT5
2012-05-19	56067.50	33.0	...	22.210 (032)	19.951 (031)	DUPONT
2012-08-10	56149.91	115.4	21.029 (035)	...	NTT
2012-08-25	56164.87	130.4	22.683 (160)	21.354 (023)	20.427 (020)	NTT
2012-09-09	56180.89	146.4	23.431 (560)	21.716 (286)	20.932 (250)	NTT
2012-10-16	56217.81	183.3	23.762 (270)	22.514 (256)	21.721 (174)	NTT
2012-11-15	56246.73	212.2	22.838 (083)	22.005 (081)	NTT
2012-12-04	56265.82	231.3	23.020 (204)	...	NTT
2012-12-06	56267.81	233.3	23.470 (217)	22.607 (145)	NTT

^a The errors are computed taking into account both the uncertainty of the PSF fitting of the SN magnitude and the uncertainty due to the background contamination (computed by an artificial-star experiment). ^b Relative to the *R*-band maximum (JD = 2,456,034.5). ^c PROMPT = PROMPT Telescopes and CCD camera Alta U47UV E2V CCD47-10; pixel scale = 0.590 arcsec pixel^{−1}. NTT = New Technology Telescope and EFOSC2; pixel scale = 0.24 arcsec pixel^{−1}. TRAPPIST = TRAnsiting Planets and Planetesimals Small Telescope and FLI CCD; pixel scale = 0.64 arcsec pixel^{−1}. DUPONT = 2.5-m du Pont telescope and SITe2k; pixel scale = 0.259 arcsec pixel^{−1}.

Table A2. Optical photometry of SN 2012hn (AB magnitudes in Sloan system)^a.

Date	JD − 2,400,000	Phase ^b	<i>g</i>	<i>r</i>	<i>i</i>	<i>z</i>	Source ^c
2012-04-14	56031.51	−3.0	18.367 (069)	NTT
2012-04-14	56031.51	−3.0	18.398 (138)	NTT
2012-04-15	56032.59	−1.9	...	17.667 (200)	PROMPT 5
2012-04-20	56037.53	3.0	18.821 (085)	17.614 (092)	17.198 (061)	16.972 (039)	PROMPT 5/3
2012-04-21	56038.52	4.0	18.882 (069)	NTT
2012-04-21	56038.53	4.0	18.852 (066)	NTT
2012-04-24	56041.48	7.0	19.276 (157)	17.760 (170)	PROMPT 5/3
2012-04-30	56048.48	14.0	19.907 (110)	18.425 (071)	17.852 (025)	17.485 (035)	NTT

^a The errors are computed taking into account both the uncertainty of the PSF fitting of the SN magnitude and the uncertainty due to the background contamination (computed by an artificial-star experiment). ^b Relative to the *R*-band maximum (JD = 2,456,034.5). ^c PROMPT = PROMPT Telescopes and CCD camera Alta U47UV E2V CCD47-10; pixel scale = 0.590 arcsec pixel^{−1}. NTT = New Technology Telescope and EFOSC2; pixel scale = 0.24 arcsec pixel^{−1}.

Table A3. Optical photometry of SN 2012hn reference stars (Vega magnitudes in Landolt system)^a.

Id	<i>U</i>	<i>B</i>	<i>V</i>	<i>R</i>	<i>I</i>
1	16.909 (068)	16.346 (021)	15.454 (017)	14.941 (020)	14.453 (017)
2	17.390 (033)	17.400 (053)	16.783 (065)	16.424 (074)	16.000 (073)
3	17.565 (043)	17.075 (059)	16.207 (089)	15.724 (083)	15.231 (091)
4	20.813 (026)	19.532 (068)	17.905 (163)	16.420 (107)	14.637 (085)
5	16.323 (025)	16.326 (060)	15.781 (083)	15.471 (086)	15.109 (059)
6	17.873 (074)	17.921 (029)	17.461 (053)	17.161 (053)	16.833 (026)
7	17.258 (051)	16.907 (005)	16.064 (020)	15.593 (031)	15.110 (024)
8	15.594 (035)	15.613 (011)	15.002 (024)	14.639 (029)	14.275 (045)
9	19.894 (075)	18.684 (046)	17.210 (029)	16.248 (023)	15.160 (032)
10	16.912 (046)	16.990 (035)	16.467 (070)	16.135 (063)	15.777 (067)

^aThe uncertainties are the standard deviation of the mean of the selected measurements.

Table A4. Optical photometry of SN 2012hn reference stars (AB magnitudes in Sloan system)^a.

Id	<i>g</i>	<i>r</i>	<i>i</i>	<i>z</i>
1	15.74 (07)	15.15 (06)	14.89 (04)	14.71 (02)
2	16.86 (07)	16.48 (06)	16.31 (04)	16.27 (02)
3	16.41 (06)	15.79 (06)	15.52 (04)	15.41 (02)
4	18.36 (07)	16.85 (06)	15.30 (03)	14.39 (02)
5	15.82 (06)	15.49 (05)	15.40 (03)	15.38 (02)
6	17.52 (07)	17.26 (06)	17.22 (04)	17.19 (02)
7	16.28 (06)	15.75 (05)	15.51 (04)	15.42 (02)
8	15.12 (06)	14.79 (05)	14.64 (03)	14.59 (02)
9	17.89 (07)	16.66 (06)	15.78 (04)	15.32 (02)
10	16.51 (07)	16.17 (06)	16.06 (04)	16.05 (02)

^aThe uncertainties are the standard deviation of the mean of the selected measurements.